

Hydraulic Fracturing Growth in Fracture Reservoirs Using Analytical and Numerical Simulation: T-Type Intersections

Jaber Taheri Shakib^{*1}, Hossein Jalalifar²

¹Department of Petroleum Engineering, Shahid Bahonar University of Kerman, Iran
Young Researchers Society

²Department of Petroleum Engineering, environmental and energy research center, Shahid Bahonar University of Kerman, Iran

(Received 20 November 2012, Accepted 1 August 2013)

Abstract

Hydraulic fracture diagnostics have highlighted the potentially complex natural of hydraulic fracture geometry and propagation. This has been particularly true in the cases of hydraulic fracture growth in naturally fractured reservoirs, where the induced fractures interact with pre-existing natural fractures. A simplified analytical and numerical model has been developed to account for mechanical interaction between induced and natural fractures. Analysis of the distance between natural fractures indicates that induced shear and tensile may be high enough to debond sealed natural fractures ahead of the arrival of the hydraulic fracture tip. We present a complex hydraulic fracture pattern propagation model based on the Extended Finite Element Method (XFEM) as a design tool that can be used to optimize treatment parameters under complex propagation conditions. Results demonstrate that fracture pattern complexity is strongly controlled by the magnitude of anisotropy of in situ stresses, and natural fracture cement strength as well as the orientation of the natural fractures relative to the hydraulic fracture.

Keywords: Shear, Tensile, Intersection, Induced Fracture, Distance.

1. Introduction

During the last decade, hydraulic fracturing has become a popular procedure to enhance production in fractured reservoir. Production improvement depends mainly on the geometry of the induced and natural fractures. Complex hydraulic fracture geometry has become more evident with the widespread application of improved fracture diagnostic technology [1]. Induced fracture propagation from vertical wells has been confirmed by coring [2], while microseismic data in naturally fractured reservoirs suggests significant diversion of hydraulic fracture paths due to intersection with natural fractures. Apparent interaction between a propagating hydraulic fracture and pre-existing natural fractures seems to be the key component explaining why some reservoirs exhibit more complex behavior [3-4]. There

are several possibilities for the interaction between hydraulic and natural fractures. The likelihood of intersection between a hydraulic and natural fracture is partly a function of orientation. If the hydraulic and natural fracture directions are parallel, intersection is less likely, but there can still be interaction between close, en echelon overlaps of fractures, and the natural fractures may be reactivated by being within the process zone (region of altered stress) around the crack tip. If the natural fractures are orthogonal to the present-day hydraulic fracture direction, the propagating hydraulic fracture is likely to cross a large number of natural fractures as it propagates through the reservoir. For these cases of direct intersection, the hydraulic fracture could propagate across the natural fracture plane without deviation and without additional

* Corresponding Author: Tel: +98-9372244208

Email: Jaber_Taherishakib@Yahoo.com

leak-off, a possible outcome for strongly cemented natural fracture planes [5]. Even if the hydraulic fracture propagates across the natural fracture, the stress induced by the hydraulic fracture could open the natural fracture enough for it to divert fracturing fluid and increase the leak-off. If the fluid diverted into the natural fracture becomes significant, the natural fracture could start to propagate, creating a new strand of the fracture that could equal or eclipse the initial hydraulic fracture wing. A more extreme interaction would be where the main hydraulic fracture wing is arrested by its intersection with the natural fracture in a T-intersection. The preliminary model described here focuses on the consequence of direct T-type intersections between the hydraulic fracture. The main objective of this

paper is the investigation of the analytical and numerical of hydraulic fracturing propagation in the presence of natural fractures.

2. Analytical Results

Fracture propagation is strongly influenced by the mechanical interaction between neighboring fractures throughout the fracture growth history. This interaction is manifested by the opening or shearing of one fracture perturbing the stress field acting on other nearby fractures. The hydraulic fracture has one wing and an initial total length of 1m. The fracture toughness of the cement is assumed to be half the toughness of the intact rock. Other main input data is specified in Table 1.

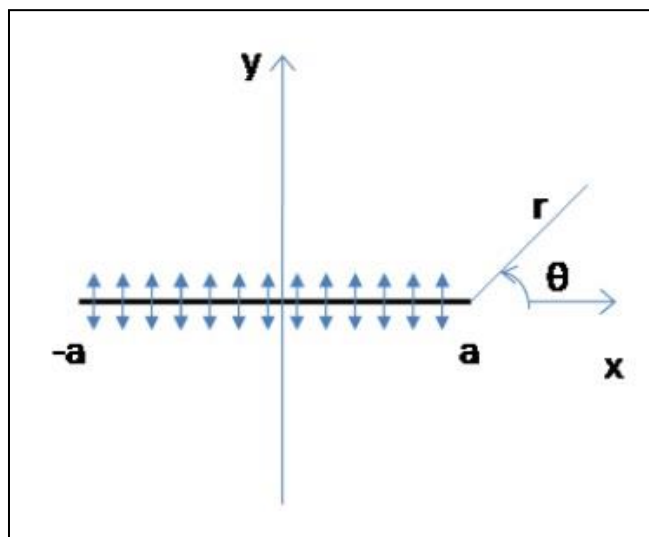


Figure 1: The geometry of a pressurized crack in an infinite plate.

Table1: Simulation data for the interaction between induced and natural fracture

Density of Intact Rock	1800 kg/m ³
Friction angle	30°
Young's modulus (E)	4.0 * 10 ⁶ psi
Poisson's ratio (ν)	0.25
Fracture toughness	1.50 MPa.m ^{1/2}
Fracture cement toughness	0.75 MPa.m ^{1/2}
Natural Fracture Length	0.5 m

Attention here is mainly focused to the interaction between the hydraulic fracture and one or two natural fractures. Fracture interaction was examined by looking at the analytical results for stress around the tip of a pressurized hydraulic fracture [6]. The normal and shear stresses for a uniformly pressurized crack of length $2a$ are:

$$\sigma_{xx} = \frac{P\sqrt{\pi a}}{\sqrt{2\pi r}} \cos \frac{\theta}{2} \left(1 - \sin \frac{\theta}{2} \sin \frac{3\theta}{2} \right) \quad (1)$$

$$\sigma_{yy} = \frac{P\sqrt{\pi a}}{\sqrt{2\pi r}} \cos \frac{\theta}{2} \left(1 + \sin \frac{\theta}{2} \sin \frac{3\theta}{2} \right) + P \quad (2)$$

$$\sigma_{xy} = \frac{P\sqrt{\pi a}}{\sqrt{2\pi r}} \sin \frac{\theta}{2} \cos \frac{\theta}{2} \cos \frac{3\theta}{2} \quad (3)$$

Where r and θ are local polar coordinates at the crack tip (Figure 1), σ_{xx} and σ_{yy} are the normal stresses parallel and normal to the crack, respectively and σ_{xy} is the shear stress. P is the pressure inside the crack. The cemented natural fracture is not actually induced in the analysis - the stresses along the location of a hypothetical crack are simply calculated. For the case where the natural fractures are orthogonal to the hydraulic fracture path, the shear and normal tractions exerted on the sealed cemented crack lying normal to the hydraulic fracture is plotted in the figure 2. The hydraulic fracture extends from west to east while the natural fracture runs from south to north. Only the part of natural fracture that is within a specific radius from the hydraulic fracture tip under tensile stress (for part (a), it is extended from -3.9 to 3.9). This observation suggests more successful results of hydraulic fracturing in reservoirs that natural fractures are orthogonal rather than parallel to the orientation of maximum horizontal stress. The shear traction peaks is slightly offset with respect to the hydraulic fracture tip at $x=2.0$ with a right lateral shear sense (positive). These results indicate that it is most likely to get opening mode fracture growth initiated ahead of the tip of an approaching hydraulic fracture. Induced

shear is more likely where shear stress magnitude peaks behind the tip, where the induced normal stress is slightly tensile. Both conditions would promote slip.

The next stages of fracture propagation after debonding are too complicated to be followed by analytical methods. This discussion is left here for later in the numerical results section. The minimum potential energy principle implies double-deflected cracks may not be produced by a simple intersection of the hydraulic fracture and sealed natural fractures, but the occurrence of debonding in the natural fractures located ahead of the primary hydraulic fracture may generate several progressive stands for the propagating fractures. This would explain the formation of the observed multi-stranded fractures.

2.1. Crack propagation criteria

Fracture propagation in linear elastic fracture mechanics (LEFM) is a function of opening and shearing mode stress intensity factors (K_I and K_{II} , respectively), which are measures of stress concentration at the tip of the crack [7]. The two stress intensity factors are combined in the energy release rate fracture propagation criterion used in this research. The energy release rate, G , is related to the stress intensity factors through Irwin's relation.

$$G = \frac{(K_I^2 + K_{II}^2)}{E^*} \quad (4)$$

where $E^* = E/(1 - \nu^2)$ for plane strain conditions (where ν is the Poisson's ratio). If the energy release rate is greater than a critical value, G_c , the fracture will propagate critically. This is the propagation criterion in the absence of chemical weakening effects that can cause "sub-critical" crack growth [8].

The direction of the fracture growth is that which maximizes the energy release rate. We can rewrite Eq. 4:

$$\bar{G} = \frac{\bar{K}_I^2}{E^*} + \frac{\bar{K}_{II}^2}{E^*} \quad (5)$$

where G is the energy release rate in a specific orientation, θ_0 , given:

$$\bar{K}_I = \frac{1}{2} \cos\left(\frac{\theta_0}{2}\right) [K_I(1 + \cos\theta_0) - 3K_{II} \sin\theta_0] \quad (6)$$

$$\bar{K}_{II} = \frac{1}{2} \cos\left(\frac{\theta_0}{2}\right) [K_I \sin\theta_0 + K_{II}(3\cos\theta_0 - 1)] \quad (7)$$

The values for k_I and k_{II} at different orientations for pure mode I loading is plotted in Figure 3.

In the case that sufficient energy is available for fracture propagation, and where a crack has more than one path to follow (Figure 4), the path most likely for it to utilize would be the path that has the maximum energy release rate, or the greater relative energy release rate [9]. The two paths can be

compared by looking at the ratios G/G_c^{rock} and G/G_c^{frac} (Figure 4), where G_c^{rock} is the rock fracture energy (proportional to the fracture toughness of unfractured rock) and G_c^{frac} is the energy required to overcome the cement strength in the pre-existing natural fractures. Fracture re-opening may happen through the cement or through the cement-matrix interface. Thus, G_c^{frac} would be the smaller of the cohesion of between the cement and intact rock and the adhesion of cement grains to each other. If G/G_c^{frac} is greatest, the pre-existing fracture will re-open. If G/G_c^{rock} is greatest, propagation will create new fracture surface following a path of $= 0 K_{II}$.

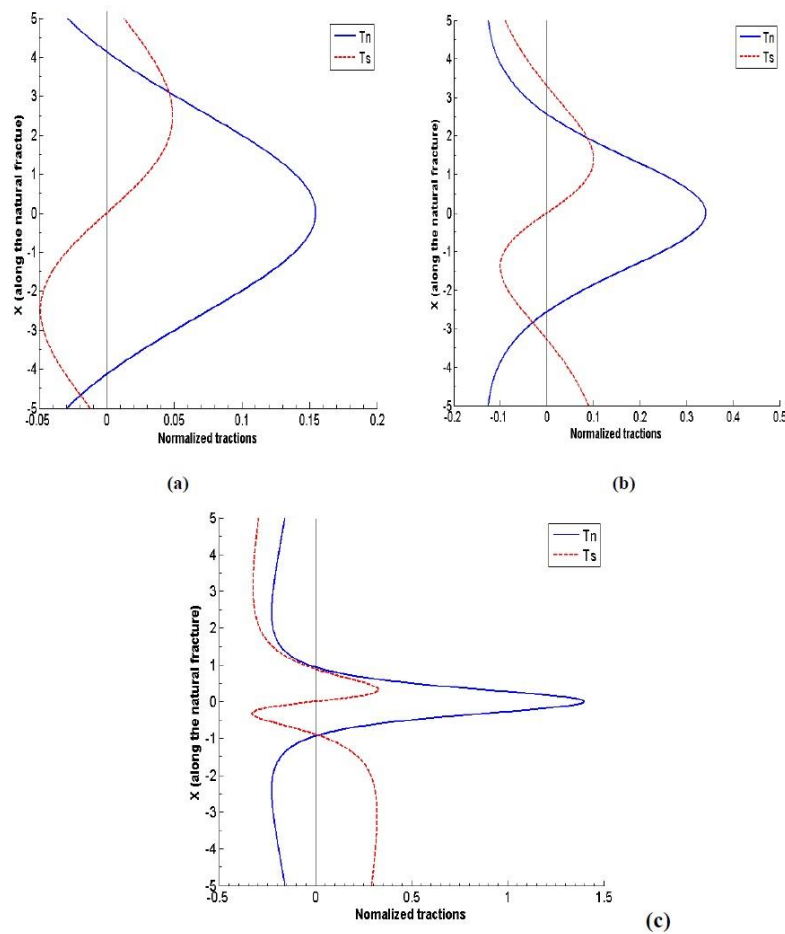


Figure 2: Normal and shear tractions ahead of the normal primary crack that are experienced by a sealed crack at distances of 1.0, 0.5 and 0.05 respectively (distances and tractions are normalized with respect to growing fracture length and pressure, respectively). These results are reproduced by XFEM results.

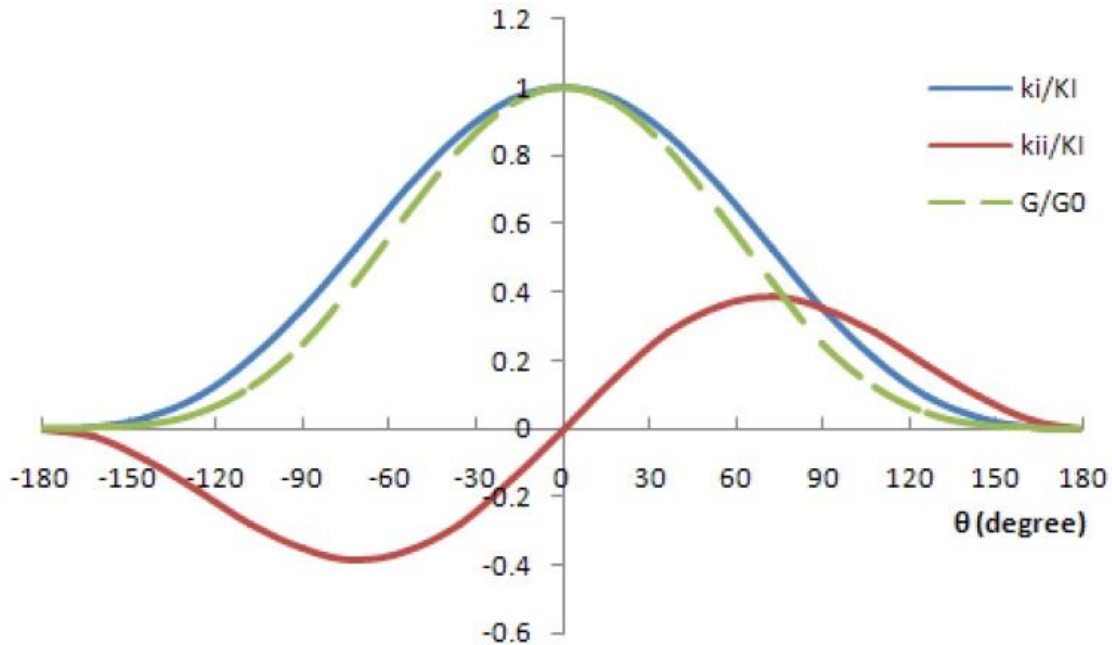
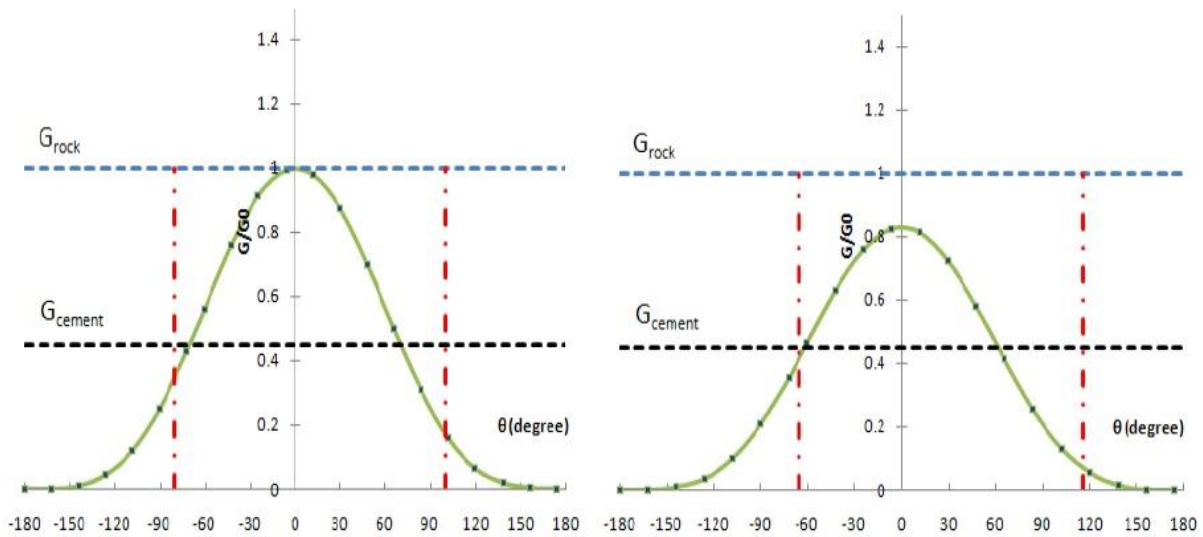


Figure 3: Values of \bar{k}_I and \bar{K}_{II} for a pure mode I case as a function of propagation direction, θ , where $\theta=0$ indicates straight propagation (expected result for pure mode I loading). The values are normalized with respect to the maximum stress intensity factor, K_I . The energy release rates in different directions are plotted (normalized with respect to its maximum value).



(a)

(b)

Figure 4: Part (a) shows an example where there is not sufficient energy release rate for fracture growth in the direction of the natural fracture shown in red line (-80 and 100 degrees), but there is sufficient energy to fracture the rock. Part (b) shows the case where the fracture will grow in one the fracture wings (oriented at -65 degree).

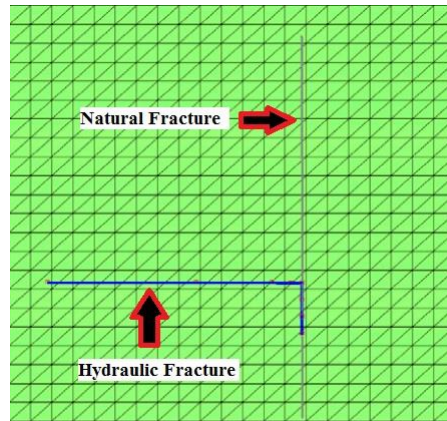


Figure 5: Hydraulic fracture diverted at normal natural fracture.

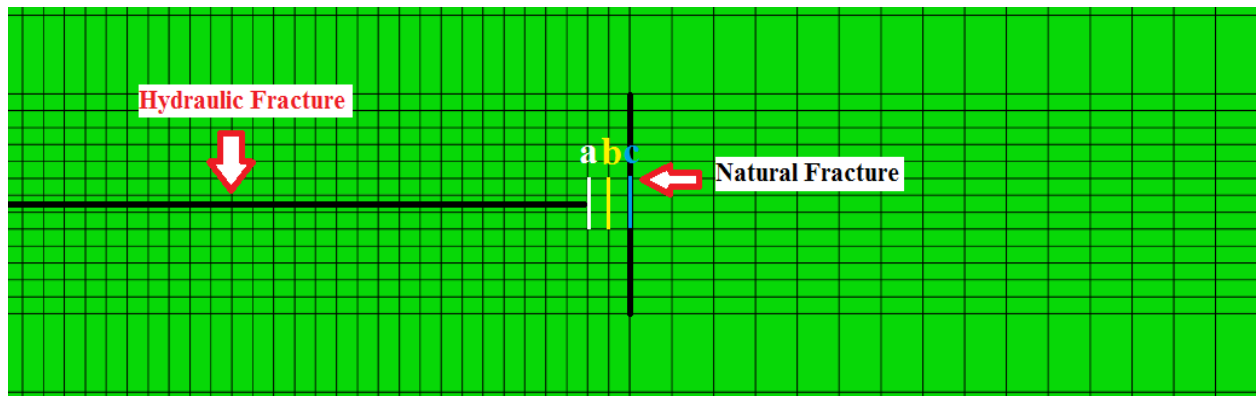


Figure 6: symmetric debonding of the sealed crack by a perpendicular primary hydraulic fracture

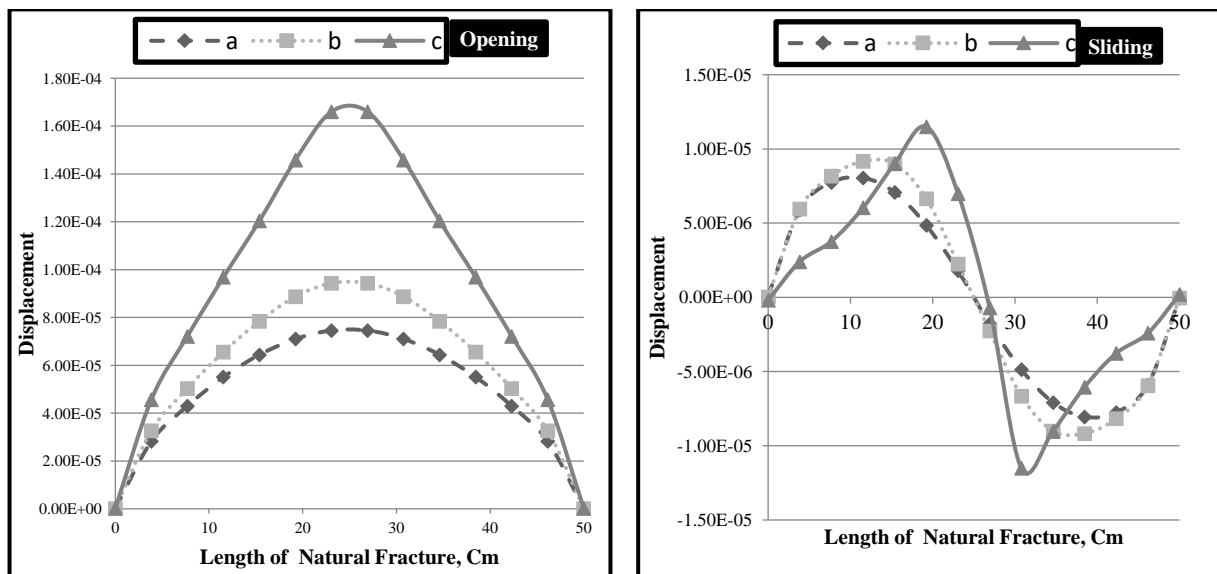


Figure 7: The opening and sliding displacements along the debonded zone of figure 6

The crack deflection into one side of the sealed crack corresponds to higher energy release rate compared to the deflection into both sides. For instance, it requires about 30% more energy to induce a double-sided fracture for the normal incidence angle case [10]. Therefore, the crack will generally deflect to one side after intersecting the sealed fracture.

3. Numerical Result

Two distinct possibilities were considered for the interactions between the hydraulic fracture and natural fractures. In the first case, it is assumed that cracks are fully-sealed by cement and will not debonded before intersection with the approaching crack. The threshold of the cement fracture toughness is verified. Below this threshold, the approaching cracks will be diverted by the natural fractures, while above that natural fractures will not affect fracture growth direction. For the case of normal intersection, it is found that threshold for G_c^{frac}/G_c^{rock} is 0.25 for fracture to be diverted along the path of the existing crack. This value matches the analytical solution proposed by He and Hutchinson (1989) [11] for interface cracks. The calculated threshold is independent of the rock elastic properties. This value is independent of the loading condition and matrix elastic properties. The threshold is strongly dependent on the angle of the intersection.

Performing hydraulic fracture design calculations under these complex conditions

requires modeling of fracture intersections and tracking fluid fronts in the network of reactivated fissures. In this dissertation, the effect of the cohesiveness of the sealed natural fractures and the intact rock toughness in hydraulic fracturing are studied. Accordingly, the role of the pre-existing fracture geometry is also investigated. The results provide some explanations for significant difference in hydraulic fracturing in naturally fractured reservoirs from non-fractured reservoirs. For the purpose of this study, an extended finite element method (XFEM) code is developed to simulate fracture propagation, initiation and intersection. The motivation behind applying XFEM are the desire to avoid remeshing in each step of the fracture propagation, being able to consider arbitrary varying geometry of natural fractures and the insensitivity of fracture propagation to mesh geometry. New modifications are introduced into XFEM to improve stress intensity factor calculations, including fracture intersection criteria into the model and improving accuracy of the solution in near crack tip regions.

The opening and sliding displacements along the debonded crack is shown in Figures 6-7. It is remarkable that the debonding length and stress intensity factors at the tips of the primary fracture or new initiated fracture are independent of the rock stiffness, because the stress field of the growing fracture is independent of rock elastic properties.

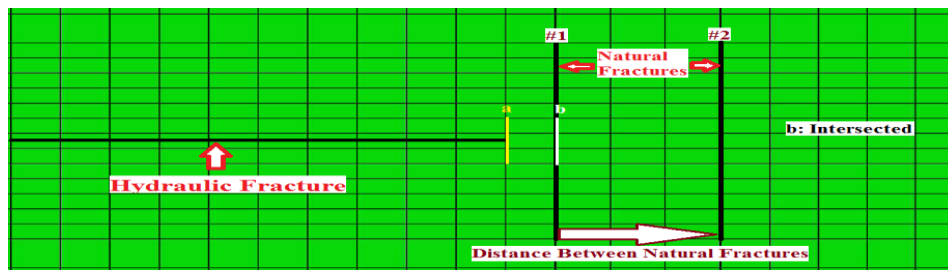


Figure 8: symmetric debonding of the two sealed cracks by a perpendicular primary hydraulic fracture

Distance Between Natural Fractures :5 Cm

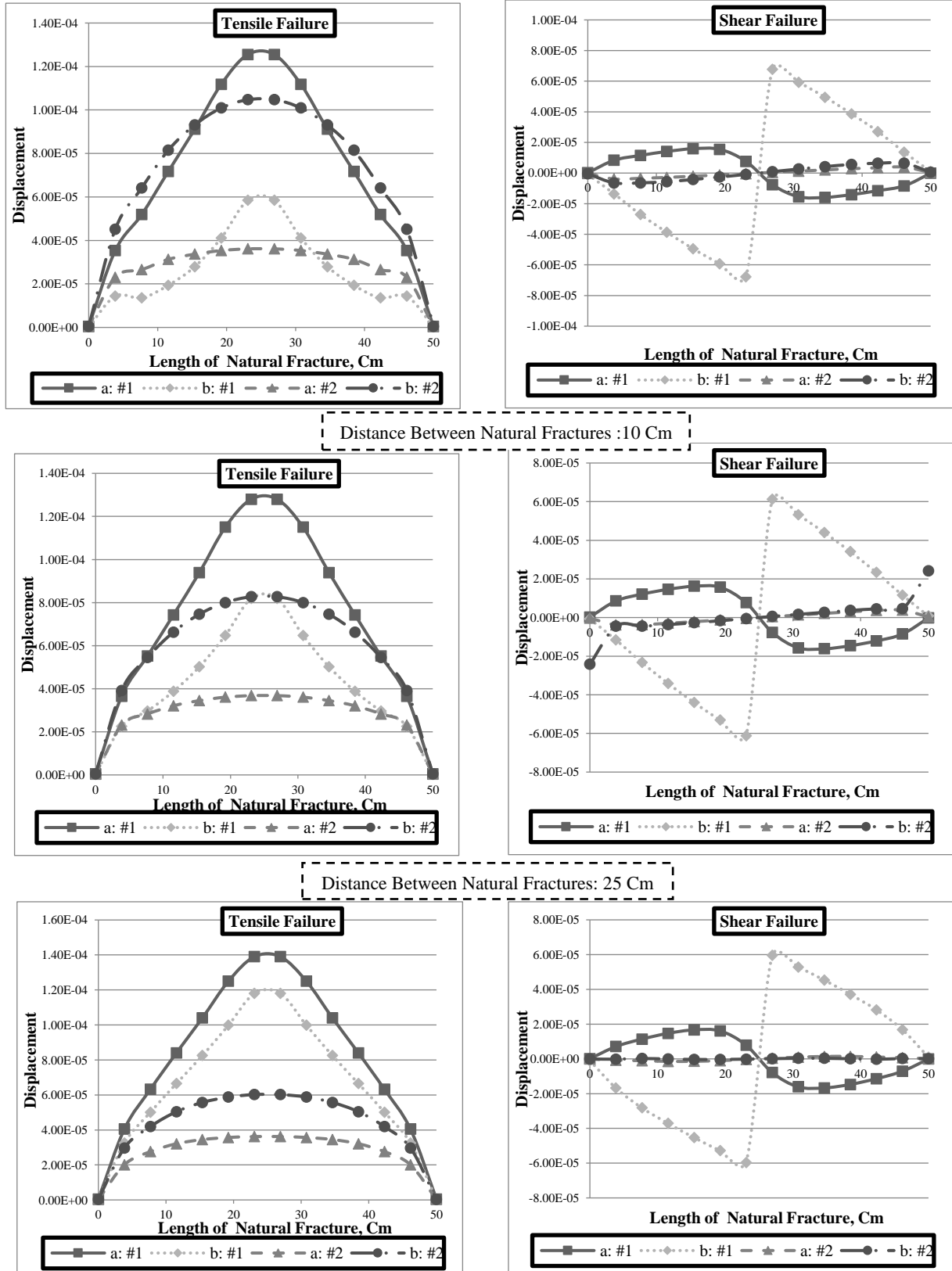


Figure 9: The opening and sliding displacements along the debonded zone of figure 8

The tensile and shear failure along the debonded zone of two natural fractures with different displacement shown in Figures 8-10.

If the hydraulic fracture intersects the natural fracture, the hydraulic fracture is arrested and the fluid is completely diverted into the natural fracture system. The natural fractures will open and/or shear if the energy of the growing hydraulic fracture is large enough to overcome the resolved normal stress, break the fracture cements, and/or overcome the friction between fracture surfaces. In the third scenario, both the hydraulic fracture crosses the natural fracture but the natural fracture is also reactivated and propagates in some complex manner.

Debonding, reopening or shearing of a natural fracture can also take place ahead of the hydraulic fracture tip prior to intersection. The hydraulic fracture exerts large tensile and shear stresses ahead of and near its tip. For instance, the induced tension on the natural fracture increases as the hydraulic fracture approaches, and the stress magnitude can be many times the net pressure of the hydraulic fracture, large enough to debond even a sealed natural fracture.

For the case of two natural fracture, the induced debonding is asymmetric with respect to the approaching crack and distance between natural fractures, may possibly become partly closed under the effect of the approaching fracture. In two natural fractures case, shear failure plays a significant rule in activating the fractures and forming asymmetric debonding with respect to the approaching crack. This observation can be justified by comparing Figure 9 with different distance, where two natural fracture amplifies the distance between natural fractures exerted on the debonding. Shear or tensile debonded zones are not necessarily intersected by the advancing hydraulic fracture.

The next stages of fracture propagation after debonding is complicated as the fracture propagation will be dominated by many factors such as anisotropy of tectonic stresses and the size and orientation of the debonded length with respect to the tip of hydraulic fracture [12].

4. Conclusion

The intersection between a growing hydraulic fracture and the surrounding natural fractures was studied. Analytical and numerical criterion were proposed to predict interaction between one and two natural fractures with respect to the hydraulic fracture. The growing fracture exerts large tensile and shear stresses ahead of and near the tip. These stresses can be large enough to debond or shear even sealed natural fractures. Analytical solution was shown that the growing hydraulic fracture exerts shear and tensile stresses on cemented cracks even before intersecting them. Depending on cemented fracture toughness, the shear and/or tensile components of stress may debond the cemented fractures before the incident crack reaches the cemented fracture. This mechanism does not necessarily cause any opening, but debonded fractures can be reopened by the intersecting crack much easier than the bonded fractures.

To be able to study interaction between hydraulic fracture and natural fractures, an extended finite element (XFEM) code was developed. It was shown that the distance between natural fractures the effect on the hydraulic fracturing propagation and debonding. The finding in this research can be used to explain different observation of hydraulic fracturing in fractured reservoirs. It gives the ability to predict the possible reactivations of natural fractures and the potential of the reactivation process. Generally, these techniques can be utilized to modify hydraulic fracturing treatment and associated design and diagnostic techniques.

Reference

- 1- Fisher, M.K., C.A. Wright, B.M. Davidson, A.K. GOODWIN, E.O. Fielder, W.S. Buckler and N.P. Steinsberger. (2005). "Interaction Fracture-mapping Technologies To Improve stimulations in the Barnett Shale". *SPE Prod and Fac.* pp. 85-93.
 - 2- Warpinski, N.R., J.C. Lorenz, P.T. Branagan, F.R. Myal, and B.L. Gall. (1993). "Examination of a cored hydraulic fracture in a deep gas well". *SPE Prod and Fac.* pp.150-158.
 - 3- Taheri Shakib, J. Ghaderi, A. Abbaszadeh shahri, A. (2012). "Analysis of hydraulic fracturing in fractured reservoir: interaction between hydraulic fracture and natural fractures". *Life Science Journal*, vol. 9(4). pp. 1854-1862.
 - 4- Gale, J.F.W., R.M. Reed, and J. Holder. (2007). "Natural fractures in the Barnett Shale and their Importance for Hydraulic Fracture Treatments". *AAPG Bulletin*. vol. 91. pp. 603-622.
 - 5- Jon E. Olson and Dahi-Taleghani, Arash. (2009). "Modeling Simultaneous Growth of Multiple Hydraulic Fractures and Their Interaction with Natural Fractures". *SPE 119739*. This paper presented at the SPE Hydraulic Fracturing Technology Conference held in The Woodlands, Texas, USA, 19–21 January.
 - 6- Pollard, D.D., Segall, P. and P.T. Delaney, (1982). "Formation and interpretation of dilatant echelon cracks." *Geological society of America Bulletin*, Des 1982; vol. 93. pp. 1291-1303.
 - 7- Lawn, B. (2004). "Fracture of Brittle Solids." *Cambridge University Press*.
 - 8- Atkinson, B. K. (1989). "Fracture Mechanics of Rock." *1st edition, Academic Press*.
 - 9- Freund, L.B. and S. Suresh. (2003). "Thin Film Material: Stress, Defect Formation, and Surface Evolution." *Cambridge University Press*.
 - 10- Arash Dahi-Taleghani and Jon E. Olson., (2009). "Numerical Modeling of Multi-Stranded Hydraulic Fracture Propagation: Accounting for the Interaction Between Induced and Natural Fractures." *SPE 124884*. This paper presented at the SPE Annual Technical Conference and Exhibition held in New Orleans, Louisiana, USA, 4–7 October.
 - 11- He, M.Y. and J.W. Hutchinson. (1989). "Crack Deflection at an Interface Between Dissimilar Elastic Materials." *International journal of solids and structures*, Vo. 25. No. 9. pp.1053-1067.
 - 12- Talaghani, A.D. (2009). "Analysis of hydraulic fracturing propagation of fractured reservoirs: an improved model for the interaction between induced and natural fracture." *PhD Thesis*, University of Texas at Austin.
-